Nitrosyl N–O Bond Cleavage Induced by Reducing Agents. Synthesis and Characterization of Novel Nitrido-Bridged Bimetallic Complexes of Molybdenum and Tungsten[1]

Jeff D. Debad, Peter Legzdins,* Roser Reina,[2] and Michelle A. Young

Department of Chemistry, The University of British Columbia, Vancouver, British Columbia, Canada V6T 1Z1

Raymond J. Batchelor and Frederick W. B. Einstein*

Department of Chemistry, Simon Fraser University, Burnaby, British Columbia, Canada V5A 1S6

Received April 29, 1994[⊗]

Reduction of Cp*W(NO)(R)Cl (Cp* = η^5-C_5Me_5; R = CH_2CMe_3, CH_2SiMe_3, Ph) with an excess of zinc powder in THF results in the formation of [Cp*W(NO)(R)](μ-N)[Cp*W(O)(R)] [R = CH_2CMe_3 (**1**), CH_2SiMe_3 (**2**), Ph (**3**)], which are isolable in good yields. Similar treatment of a 2:1 mixture of Cp*W(NO)(CH_2CMe_3)Cl and Cp*W(NO)Cl_2 affords the related bimetallic complex, [Cp*W(NO)(CH_2CMe_3)](μ-N)[Cp*W(O)Cl] (**4**), in 24% isolated yield. In an analogous manner, exposure of C_6H_6 solutions of Cp′Mo(NO)(CH_2SiMe_3)$_2$ [Cp′ = Cp* or Cp$^\phi$ (η^5-C_5Ph_4H)] to dihydrogen results in the formation of the dimolybdenum complexes, [Cp′Mo(NO)(CH_2SiMe_3)](μ-N)[Cp′Mo(O)(CH_2SiMe_3)] [Cp′ = Cp* (**5**) or Cp$^\phi$ (**6**)], which are isolable in 40% and 53% yields, respectively. Complexes **4** and **5** have been subjected to single-crystal X-ray crystallographic analyses at 190 K. Crystals of **4** are triclinic, space group $P\bar{1}$; $Z = 2$; $a = 10.923(2)$ Å; $b = 11.328(4)$ Å; $c = 12.151(6)$ Å; $\alpha = 109.16(4)°$; $\beta = 90.88(3)°$; $\gamma = 101.92(2)°$; $V = 1384.0$ Å^3; $R_F = 0.026$ for 4268 data [$I_o \geq 2.5\sigma(I_o)$] and 278 variables. Crystals of **5** are triclinic, space group $P\bar{1}$; $Z = 2$, $a = 10.284(4)$ Å; $b = 11.043(2)$ Å; $c = 16.979(3)$ Å; $\alpha = 85.97(2)°$; $\beta = 75.29(2)°$; $\gamma = 65.70(2)°$; $V = 1698.5$ Å^3; $R_F = 0.037$ for 4422 data [$I_o \geq 2.5\sigma(I_o)$] and 331 variables. Both structures were solved by standard heavy-atom methods and were refined by full-matrix least-squares procedures. The most chemically interesting feature about the solid-state molecular structures of **4** and **5** is the orthogonal orientation of the metal-containing units about the essentially linear M–N–M (M = Mo, W) bridging linkages, an aspect consistent with the existence of multiple bonding in these linkages. It is proposed that all the bimetallic products result via transient formation of a coordinatively unsaturated Cp′M(η^2-NO)(X) (X = R or Cl) species that then combines with another molecule of the original nitrosyl reactant.

Introduction

The principal focus of our research during the past few years has been the development of organometallic nitrosyl complexes of the Group 6 elements as unique synthetic reagents.[3] During these studies we have generally found that the nitrosyl ligands remain intact during the various chemical transformations involving these compounds, thereby permitting the strong π-acidity of the NO groups to be utilized for the regulation of electron density at the metal centers. Recently, however, a new type of chemical reactivity that we are encountering with increasing frequency in these systems is that of nitrosyl N–O bond cleavage under relatively mild conditions. The examples of such cleavage that we have reported to date include (a) exposure of Cp′M(NO)R_2 complexes [Cp′ = Cp*(η^5-C_5Me_5), Cp (η^5-C_5H_5); M = Mo, W; R = alkyl, aryl] to molecular oxygen,[4] a process which yields Cp′M$(O)_2$R products, (b) the isomerization of CpW(NO)(*o*-tolyl)$_2$ to CpW(O)(N-*o*-tolyl)(*o*-tolyl), which is catalyzed by water at room temperature,[5] and (c) the thermally-induced N–O bond cleavage in Cp*W(NO)Ph_2, which produces a variety of products, the most interesting of which is Cp*W(η^2-ONPh)(NPh)Ph.[6] In this report we describe the facile nitrosyl N–O bond cleavage that occurs in some Cp′M(NO)X_2 [Cp′ = Cp* or Cp$^\phi$ (η^5-C_5Ph_4H); X = CH_2CMe_3, CH_2SiMe_3, Ph, or Cl] systems when they are exposed to reducing conditions (e.g., Zn or H_2). Our studies of these N–O cleavage processes are intended to contribute to a better understanding of the pathways by which organotransition-metal complexes can degrade or decompose, a mechanistic area that is still relatively poorly understood.[7]

⊗ Abstract published in *Advance ACS Abstracts,* September 15, 1994.

(1) Presented in part at the 75th Canadian Chemical Conference, Edmonton, Alberta, June 1992, Abstract 370P, and at the 206th ACS National Meeting, Chicago, IL, Aug 1993, Abstract INOR 466.

(2) Present address: Departament de Química Inorgánica, Universitat de Barcelona, Diagonal, 647, 08028 Barcelona, Spain.

(3) Legzdins, P.; Veltheer, J. E. *Acc. Chem. Res.* **1993**, *26*, 41.

(4) Legzdins, P.; Phillips, E. C.; Sánchez, L. *Organometallics* **1989**, *8*, 940 and references therein.

(5) Legzdins, P.; Rettig, S. J.; Ross, K. J.; Veltheer, J. E. *J. Am. Chem. Soc.* **1991**, *113*, 4361.

(6) Brouwer, E. B.; Legzdins, P.; Rettig, S. J.; Ross, K. J. *Organometallics* **1994**, *13*, 2088.

0276-7333/94/2313-4315$04.50/0

Experimental Section

All reactions and subsequent manipulations involving organometallic reagents were performed under anaerobic and anhydrous conditions in an atmosphere of purified dinitrogen or argon.[8] Conventional glovebox and vacuum-line Schlenk techniques were utilized throughout. General procedures routinely employed in these laboratories have been described in detail previously.[9] The organometallic reagents Cp*W(NO)Cl_2,[10] Cp*W(NO)(CH_2SiMe_3)Cl, Cp*W(NO)(CH_2CMe_3)Cl, Cp*W(NO)(Ph)Cl,[11] Cp$^{\phi}$Mo(NO)(CH_2SiMe_3)$_2$,[12] and Cp*M(NO)(CH_2SiMe_3)$_2$ (M = Mo, W)[4,13] were prepared by published procedures. H_2 (Linde, extra dry) and zinc powder (Fisher) were used as received.

Preparation of [Cp*W(NO)(R)](μ-N)[Cp*W(O)(R)] [R = CH_2CMe_3 (1), CH_2SiMe_3 (2), Ph (3)]. Complexes **1**, **2**, and **3** were synthesized similarly. The preparation of **1** is described as a representative example. Cp*W(NO)(CH_2CMe_3)Cl (150 mg, 0.33 mmol) and excess Zn powder (500 mg) were weighed into a Schlenk tube containing a magnetic stir bar, and THF (~10 mL) was then vacuum transferred onto the solids. The vessel was warmed to room temperature, and the reaction mixture was stirred for 5 h, whereupon its color changed from purple to green-brown. The solvent was removed in vacuo, and the residue was extracted with Et_2O (2 × 10 mL). The combined extracts were filtered through Florisil (2 × 2 cm) supported on a glass frit, and the column was washed with Et_2O until the washings were colorless. Solvent was removed from the combined filtrates in vacuo, and the brown powder remaining was dissolved in a minimum of hexanes. Cooling of the hexanes solution at −30 °C overnight induced the deposition of green-brown crystals of complex **1**. These crystals were recrystallized from hexanes to obtain analytically pure product (80 mg, 58% yield based on tungsten).

Anal. Calcd for $C_{30}H_{52}N_2O_2W_2$ (**1**): C, 42.87; H, 6.24; N, 3.33. Found: C, 42.59; H, 6.44; N, 3.29. IR (Nujol) ν_{NO} 1545 cm^{-1}; also 962, 891 cm^{-1}. ^1H NMR ($CDCl_3$) δ 2.00 (s, 15H, C_5Me_5), 1.93 (s, 15H, C_5Me_5), 1.78 (d, $^2J_{HH}$ = 14.1 Hz, 1H, CH_2), 1.49 (d, $^2J_{HH}$ = 13.2 Hz, 1H, CH_2), 1.31 (d, $^2J_{HH}$ = 14.1 Hz, 1H, CH_2), 1.13 (s, 9H, CMe_3), 1.01 (s, 9H, CMe_3), remaining CH_2 signal obscured. $^{13}C\{^1H\}$ ($CDCl_3$) δ 115.11 (C_5Me_5), 111.34 (C_5Me_5), 64.80 (CH_2), 49.99 (CH_2), 37.43 (CMe_3), 33.99 (CMe_3), 33.60 (CMe_3), 33.40 (CMe_3), 10.94 (C_5Me_5), 10.37 (C_5Me_5). Low-resolution mass spectrum (probe temperature 200 °C): *m/z* 840 [P^+].

Similar treatment of Cp*W(NO)(CH_2SiMe_3)Cl and Cp*W(NO)(Ph)Cl led to the isolation of complexes **2** and **3** as deep green crystals in 62% and 48% yields based on tungsten, respectively.

Anal. Calcd for $C_{28}H_{52}N_2O_2Si_2W_2$ (**2**): C, 38.54; H, 6.01; N, 3.21. Found: C, 38.40; H, 5.87; N, 3.11. IR (Nujol) ν_{NO} 1547 cm^{-1}; also 962, 892 cm^{-1}. ^1H NMR ($CDCl_3$) δ 2.00 (s, 15H, C_5Me_5), 1.91 (s, 15H, C_5Me_5), 0.53 (d, $^2J_{HH}$ = 12 Hz, 1H, CH_2), −0.13 (d, $^2J_{HH}$ = 11 Hz, 1H, CH_2), 0.086 (s, 9H, CMe_3), 0.017 (s, 9H, CMe_3), remaining CH_2 signals obscured. $^{13}C\{^1H\}$ ($CDCl_3$) δ 115.07 (C_5Me_5), 111.47 (C_5Me_5), 30.62 (br, CH_2), 18.17 (br, CH_2), 10.98 (C_5Me_5), 10.23 (C_5Me_5), 2.53 ($SiMe_3$), 1.27 ($SiMe_3$). Low-resolution mass spectrum (probe temperature 200 °C): *m/z* 872 [P^+].

Anal. Calcd for $C_{32}H_{40}N_2O_2W_2$ (**3**): C, 45.09; H, 4.73; N, 3.29. Found: C, 43.97; H, 4.68; N, 3.19. IR (Nujol mull): ν_{NO} 1598 cm^{-1}; also 969 cm^{-1}. ^1H NMR (C_6D_6) δ 7.94 (d, $^3J_{HH}$ = 7.8 Hz, 2H, Ar*H*), 7.70 (d, $^3J_{HH}$ = 8.0 Hz, 2H, Ar*H*), 7.35−7.15 (m, 6H, Ar*H*), 1.69 (s, 15H, C_5Me_5), 1.66 (s, 15H, C_5Me_5). Low-resolution mass spectrum (probe temperature 150 °C): *m/z* 852 [P^+].

Preparation of [Cp*W(NO)(CH_2CMe_3)](μ-N)[Cp*W(O)Cl] (4). Cp*W(NO)(CH_2CMe_3)Cl (450 mg, 0.99 mmol), Cp*W(NO)Cl_2 (210 mg, 0.50 mmol), and excess Zn powder (500 mg) were weighed into a Schlenk tube containing a magnetic stirbar. THF (~10 mL) was then vacuum transferred onto the solids. The vessel was warmed to room temperature, and the purple mixture was stirred for 20 min, during which time it became brown. Solvent was removed in vacuo, the residue was extracted with Et_2O (2 × 10 mL), and the extracts were filtered through a column of Florisil (2 × 2 cm) supported on a glass frit. The column was washed with Et_2O until the washings were colorless. The solvent was removed from the combined filtrates under reduced pressure, and the tan-colored powder remaining was dissolved in a minimum of hexanes. Cooling of the hexanes solution for 3 d at −30 °C resulted in the deposition of brown crystals of complex **4** [100 mg, 24% yield based on Cp*W(NO)Cl_2]. Single crystals of **4** suitable for X-ray difraction studies were obtained by recrystallization of this crystalline material from hexanes.

IR (Nujol) ν_{NO} 1549 cm^{-1}; also 962, 889 cm^{-1}. ^1H NMR ($CDCl_3$) δ 2.10 (s, 15H, C_5Me_5), 1.92 (s, 15H, C_5Me_5), 1.73 (d, $^2J_{HH}$ = 14.1 Hz, 1H, CH_2), 1.40 (d, $^2J_{HH}$ = 14.1 Hz, 1H, CH_2), 1.12 (s, 9H, CMe_3). $^{13}C\{^1H\}$ ($CDCl_3$) δ 118.32 (C_5Me_5), 112.35 (C_5Me_5), 69.14 ($^1J_{WC}$ = 107 Hz, CH_2), 37.69 (CMe_3), 33.72 (CMe_3), 11.06 (C_5Me_5), 10.16 (C_5Me_5). Low-resolution mass spectrum (probe temperature 120 °C): *m/z* 804 [P^+].

Preparation of [Cp*Mo(NO)(CH_2SiMe_3)](μ-N)[Cp*Mo(O)(CH_2SiMe_3)] (5). A purple solution of Cp*Mo(NO)(CH_2SiMe_3)$_2$ (0.41 g, 0.94 mmol) in C_6H_6 (20 mL) was exposed to an atmosphere of H_2 at −78 °C. The reaction mixture was stirred while being permitted to warm to room temperature over 1 h, during which time its color changed to red-brown. Solvent was removed from the final mixture in vacuo to obtain a red-brown residue which was extracted with hexanes (2 × 15 mL). The combined extracts were concentrated under reduced pressure and then chromatographed on a Florisil column (3 × 8 cm) using hexanes/Et_2O (2:1) as eluant. A green band which developed was collected, and solvent was removed from the eluate in vacuo to obtain a green residue. This residue was dissolved in a minimum of pentane, and the solution was maintained at −8 °C for 4 weeks to induce the deposition of analytically pure **5** (0.13 g, 40% yield).

Anal. Calcd for $C_{28}H_{52}N_2O_2Si_2Mo_2$: C, 48.25; H, 7.54; N, 4.02. Found: C, 48.40; H, 7.70; N, 3.99. IR (Nujol): ν_{NO} 1581 cm^{-1}; also 824, 829, 800 cm^{-1}. ^1H NMR (C_6D_6) δ 1.75 (s, 15H, C_5Me_5), 1.65 (s, 15H, C_5Me_5), 0.55 (s, 9H, $SiMe_3$), 0.40 (s, 9H, $SiMe_3$), 0.93 (br s, 2H, CH_2), 0.00 (br s, 2H, CH_2). Low-resolution mass spectrum (probe temperature 120 °C): *m/z* 698 [P^+].

Preparation of [Cp$^{\phi}$Mo(NO)(CH_2SiMe_3)](μ-N)[Cp$^{\phi}$Mo(O)(CH_2SiMe_3)] (6). A solution of Cp$^{\phi}$Mo(NO)(CH_2SiMe_3)$_2$ (0.67 g, 1.0 mmol) in C_6H_6 (20 mL) was exposed to H_2 (1 atm) at −78 °C. The reaction mixture was stirred as it was warmed for 1 h, during which time its color changed from purple to green. The final mixture was taken to dryness in vacuo, the remaining residue was extracted with Et_2O (2 × 15 mL), and the extracts were filtered through a column of Florisil (2 × 2 cm) supported on a glass frit. The Florisil column was washed with Et_2O until the washings were colorless. Solvent was removed from the combined filtrates in vacuo, and the remain-

(7) Collman, J. P.; Hegedus, L. S.; Norton, J. R.; Finke, R. G. *Principles and Applications of Organotransition Metal Chemistry*; University Science Books: Mill Valley, CA, 1987.
(8) (a) Shriver, D. F.; Drezdzon, M. A. *The Manipulation of Air-Sensitive Compounds*, 2nd ed.; Wiley-Interscience: New York, 1986. (b) Wayda, A. L.; Darensbourg, M. Y. *Experimental Organometallic Chemistry: A Practicum in Synthesis and Characterization*; ACS Symposium Series 357; American Chemical Society: Washington, DC, 1987.
(9) Dryden, N. H.; Legzdins, P.; Rettig, S. J.; Veltheer, J. E. *Organometallics* **1992**, *11*, 2583.
(10) Dryden, N. H.; Legzdins, P.; Batchelor, R. J.; Einstein, F. W. B. *Organometallics* **1991**, *10*, 2077.
(11) Debad, J. D.; Legzdins, P.; Batchelor, R. J.; Einstein, F. W. B. *Organometallics* **1993**, *12*, 2094.
(12) Legzdins, P.; Reina, R.; Shaw, M. J.; Batchelor, R. J.; Einstein, F. W. B. *Organometallics* **1993**, *12*, 1029.
(13) Legzdins, P.; Lundmark, P. J.; Phillips, E. C.; Rettig, S. J.; Veltheer, J. E. *Organometallics* **1992**, *11*, 2991.

ing residue was recrystallized from CH_2Cl_2/hexanes at −8 °C to obtain 0.31 g (53% yield) of analytically pure **6** as a green solid.

Anal. Calcd for $C_{66}H_{64}N_2O_2Si_2Mo_2$: C, 68.05; H, 5.49; N, 2.40. Found: C, 67.92; H, 5.33; N, 2.24. IR (Nujol): ν_{NO} 1616 cm^{-1}; also 881, 858, 842 cm^{-1}. ^1H NMR (C_6D_6) δ 7.75 (m, 40H, C_5Ph_4H), 4.24 (s, 2H, C_5Ph_4H), 1.71 (d, $^2J_{HH}$ = 10.2 Hz, 1H, CH_2), 0.91 (d, $^2J_{HH}$ = 12.3 Hz, 1H, CH_2), 0.42 (d, $^2J_{HH}$ = 10.5 Hz, 1H, CH_2), 0.33 (d, $^2J_{HH}$ = 12.6 Hz, 1H, CH_2), 0.10 (s, 9H, $SiMe_3$), 0.07 (s, 9H, $SiMe_3$). FAB mass spectrum: *m/z* 1167 [P^+ − Cp^*Mo].

X-ray Crystallographic Analyses of [Cp*W(NO)(CH_2CMe_3)](μ-N)[Cp*W(O)Cl] (4) and [Cp*Mo(NO)CH_2SiMe_3)](μ-N)[Cp*Mo(O)(CH_2SiMe_3)] (5). Crystals of **4** were gently wedged in glass capillaries using Apiezon grease as adhesive. A crystal of **5** was mounted on a glass fiber using epoxy adhesive. Data were recorded at 190 K with an Enraf Nonius CAD4F diffractometer using graphite monochromatized Mo Kα radiation and an in-house modified low-temperature attachment. Two standard reflections were measured each hour and fluctuated in intensity (~±2%) in either case. In the case of **4**, the crystal became dislodged after approximately 60% of the data had been collected, and a second crystal (of comparable size and shape) which yielded indistinguishably different cell dimensions was used to complete the intensity measurements. The data were corrected for absorptions by the Gaussian integration method,[14] and the corrections were carefully checked against measured ψ scans for data obtained with each crystal. Data reduction included corrections for Lorentz and polarization effects. The programs used for absorption corrections, data reduction, structure solution, and graphical output were from the *NRCVAX* crystal structure system.[15] Refinement was carried out using *CRYSTALS*.[16] Complex scattering factors for neutral atoms[17] were used in the calculation of structure factors. Weighting schemes based on counting statistics for which $\langle w(|F_o| - |F_c|)^2\rangle$ was nearly constant as a function of both $|F_o|$ and (sin θ)/λ were used. Computations were carried out on Micro VAX-II and 80486 computers. Crystallographic details for both complexes are summarized in Table 1.

For complex **4**, independent scale factors were refined for the data from the two crystals used. Anisotropic displacement parameters, restrained to have nearly zero net differences in the along-bond components for pairs of mutually bonded atoms, were refined for all non-hydrogen atom sites. Extremely anisotropic displacement parameters for one of the Cp* groups [bound to W(2)] were consistent with disordered orientations of this group about the W—Cp*—center-of-mass axis. This observation was not an artifact of the use of two different crystals, since it was also observed when only data from the first crystal were used. With the use of reasonable dimensional restraints, and isotropic atomic displacement parameters constrained to be equal for each disordered pair of carbon atom sites, an equally disordered model was developed which involved two orientations for the Cp* group. Later, a relative fractional occupancy was refined. Hydrogen atoms with appropriate occupancies were included in calculated positions [d(C—H) = 0.95 Å] and with isotropic displacement parameters initially proportional to the isotropic or equivalent displacement parameters for the carbon atoms to which they were bound. The hydrogen atoms were made to ride on their respective carbon atoms during refinement. A mean isotropic displacement parameter for each set of chemically equivalent hydrogen atoms was refined. Subsequently, the disordered Cp* was refined as two rigid groups including all C and H atoms for each orientation. Anisotropic displacement parameters, constrained to be equal for each pair of disordered carbon atoms, were then included. An extinction parameter [0.20(2) μm][18] was also refined. The final full-matrix least-squares refinement of 278 parameters for 4268 observations and 56 restraints converged (maximum |shift/esd| = 0.03) at R = 0.026. The maximum peak in the final difference map [1.2(2) e $Å^{-3}$] occurred 0.96 Å from W(2).

Table 1. Crystallographic Data for the Structure Determinations of [Cp*W(NO)(CH_2CMe_3)](μ-N)-[Cp*W(O)Cl] (4) and [Cp*Mo(NO)(CH_2SiMe_3)](μ-N)-[Cp*Mo(O)(CH_2SiMe_3)] (5)

	4	5
formula	$W_2ClO_2N_2C_{25}H_{41}$	$Mo_2Si_2O_2N_2C_{28}H_{52}$
cryst syst	triclinic	triclinic
mol wt	804.76	696.78
space group	$P\bar{1}$	$P\bar{1}$
a (Å)[a]	10.923(2)	10.284(4)
b (Å)	11.328(4)	11.043(2)
c (Å)	12.151(6)	16.979(3)
α (deg)	109.16(4)	85.97(2)
β (deg)	90.88(3)	75.29(2)
γ (deg)	101.92(2)	65.70(2)
V (Å^3)	1384.0	1698.5
T (K)	190	190
Z	2	2
ϱ_c (g cm^{-3})	1.931	1.362
λ(Mo Kα$_1$) (Å)	0.70930	0.70930
μ(Mo Kα) (mm^{-1})	8.605	0.81
cryst size (mm)	0.18 × 0.22 × 0.22[b] 0.20 × 0.21 × 0.24[c]	0.20 × 0.24 × 0.26
transmission[d]	0.152−0.284	0.839−0.868
2θ range (deg)	4−50	4−48
R_F[e]	0.026	0.037
R_{wF}[f]	0.041	0.051

[a] Cell dimensions were determined in each case from 25 reflections (**4**: 40° ≤ 2θ ≤ 50°; **5**: 36° ≤ 2θ ≤ 44°). [b] Crystal no. 1: measured 4° ≤ 2θ ≤ 30° and 30° ≤ 2θ ≤ 50°, k = 0 to k = 5 inclusive. [c] Crystal no. 2: measured 30° ≤ 2θ ≤ 50° and k > 5. [d] The data were corrected by the Gaussian integration method for the effects of absorption. [e] $R_F = \sum||F_o| - |F_c||/\sum|F_o|$, for 4268 (**4**) and 4422 (**5**) data [$I_o \geq 2.5\sigma(I_o)$]. [f] $R_{wF} = [\sum(w(|F_o| - |F_c|)^2/\sum(wF_o^2)]^{1/2}$ for observed data (see footnote e); $w = [\sigma(F_o)^2 + kF_o^2]^{-1}$; **4**, k = 0.0002; **5**, k = 0.0004.

For complex **5**, anisotropic displacement parameters were refined for the non-hydrogen atom sites. Hydrogen atoms were included in calculated positions [d(C—H) = 0.95 Å] and with isotropic displacement parameters initially proportional to the equivalent isotropic displacement parameters of the carbon atoms to which they were bound. The hydrogen atoms were made to ride on their respective carbon atoms during refinement. A mean isotropic displacement parameter for each set of chemically equivalent hydrogen atoms was refined and its shift applied to the individual hydrogen atom displacement parameters. The final full-matrix least-squares refinement of 331 parameters for 4422 observations converged (maximum |shift/esd| = 0.03) at R = 0.037. The maximum peak in the final difference map [1.0(2) e $Å^{-3}$] occurred 0.94 Å from Mo(2).

The atomic coordinates and equivalent isotropic temperature factors for non-hydrogen atoms of both complexes are listed in Tables 2 and 3. Selected bond lengths (Å) and bond angles (deg) for the complexes are presented in Tables 4 and 5. Hydrogen atom parameters, anisotropic thermal parameters, additional bond lengths and angles, torsion angles, and least-squares planes are provided as supplementary material. Views of the solid-state molecular structures of complexes **4** and **5** are presented in Figures 1 and 2, respectively.

(14) Busing, W. R.; Levy, H. A. *Acta Crystallogr.* **1957**, *10*, 180.
(15) Gabe, E. J.; LePage, Y.; Charland, J.-P.; Lee, F. L.; White, P. S. NRCVAX—An Interactive Program System for Structure Analysis. *J. Appl. Crystallogr.* **1989**, *22*, 384.
(16) Watkin, D. J.; Carruthers, J. R.; Betteridge, P. W. CRYSTALS, Chemical Crystallography Laboratory, University of Oxford, Oxford, England, 1984.
(17) *International Tables for X-ray Crystallography*; Kynoch Press: Birmingham, England, 1975; Vol. IV, p 99.
(18) Larson, A. C. In *Crystallographic Computing*; Ahmed, F. R., Ed.; Munksgaard: Copenhagen, 1970; p 293.

Table 2. Fractional Coordinates and Equivalent Isotropic Displacement Parameters (Å²) for the Non-hydrogen Atoms of [Cp*W(NO)(CH₂CMe₃)](μ-N)[Cp*W(O)Cl] (4) at 190 K

atom	x	y	z	U_{eq}[a]
W(1)	0.28818(2)	0.67888(2)	0.32397(2)	0.0203
W(2)	0.27920(2)	0.94737(2)	0.21416(2)	0.0212
Cl	0.23884(15)	1.10552(14)	0.38054(12)	0.0335
O(1)	0.2087(5)	0.4507(5)	0.1070(4)	0.0470
O(2)	0.4329(4)	1.0028(4)	0.1951(4)	0.0316
N(1)	0.2496(5)	0.5495(5)	0.1908(4)	0.0278
N(2)	0.2805(4)	0.8179(4)	0.2698(3)	0.0208
C(6)	0.4856(5)	0.6763(6)	0.3435(5)	0.0283
C(7)	0.5642(6)	0.6424(6)	0.2386(5)	0.0309
C(8)	0.5279(7)	0.5023(7)	0.1661(6)	0.0455
C(9)	0.5522(7)	0.7223(7)	0.1607(6)	0.0387
C(10)	0.7013(6)	0.6763(9)	0.2863(7)	0.0454
C(1)	0.3035(5)	0.6811(6)	0.5255(5)	0.0256
C(2)	0.2222(6)	0.5653(6)	0.4540(5)	0.0291
C(3)	0.1177(6)	0.5981(6)	0.4080(5)	0.0294
C(4)	0.1341(6)	0.7338(6)	0.4573(5)	0.0300
C(5)	0.2506(6)	0.7847(6)	0.5255(5)	0.0276
C(11)	0.4177(6)	0.6893(6)	0.5998(5)	0.0324
C(12)	0.2370(7)	0.4316(6)	0.4298(6)	0.0423
C(13)	0.0043(6)	0.5026(7)	0.3347(6)	0.0429
C(14)	0.0434(6)	0.8105(7)	0.4397(6)	0.0381
C(15)	0.3056(7)	0.9248(6)	0.5936(6)	0.0397
C(21)[b]	0.2263	1.0023	0.0492	0.0285
C(22)[b]	0.1249	1.0282	0.1179	0.0293
C(23)[b]	0.0567	0.9112	0.1269	0.0276
C(24)[b]	0.1150	0.8120	0.0648	0.0280
C(25)[b]	0.2213	0.8677	0.0174	0.0293
C(31)[b]	0.3180	1.0945	0.0066	0.0533
C(32)[b]	0.0883	1.1559	0.1651	0.0483
C(33)[b]	−0.0605	0.8971	0.1895	0.0476
C(34)[b]	0.0680	0.6713	0.0499	0.0493
C(35)[b]	0.3046	0.7942	−0.0635	0.0534
C(41)[c]	0.2299	0.9515	0.0224	0.0285
C(42)[c]	0.1521	1.0236	0.0962	0.0293
C(43)[c]	0.0660	0.9377	0.1373	0.0276
C(44)[c]	0.0919	0.8141	0.0909	0.0280
C(45)[c]	0.1955	0.8239	0.0226	0.0293
C(51)[c]	0.3321	1.0041	−0.0436	0.0533
C(52)[c]	0.1517	1.1641	0.1230	0.0483
C(53)[c]	−0.0397	0.9692	0.2100	0.0476
C(54)[c]	0.0211	0.6893	0.1023	0.0493
C(55)[c]	0.2513	0.7148	−0.0497	0.0534

[a] The equivalent isotropic displacement parameter is the cube root of the product of the principal axes of the anisotropic displacement ellipsoid. [b] Site occupancy = 0.281(12). [c] Site occupancy = 1 − 0.281(12) = 0.719.

Results and Discussion

Preparation of the Bimetallic Complexes [Cp′M(NO)(R)](μ-N)[Cp′M(O)(R)] (Cp′ = Cp* or Cp^ϕ; M = Mo or W; R = CH₂CMe₃, CH₂SiMe₃, or Ph). Treatment of Cp*W(NO)(CH₂CMe₃)Cl in THF with excess Zn powder produces the bimetallic complex [Cp*W(NO)(CH₂CMe₃)](μ-N)[Cp*W(O)(CH₂CMe₃)] (**1**), which is isolable as green-brown crystals in 58% yield based on W from the final reaction mixture. The analogous bimetallic products are obtained in comparable yields when Cp*W(NO)(CH₂SiMe₃)Cl and Cp*W(NO)(Ph)Cl are treated similarly (eq 1). We have obtained the phenyl-containing complex, **3**, previously in low yields by thermolysis of Cp*W(NO)Ph₂.[6]

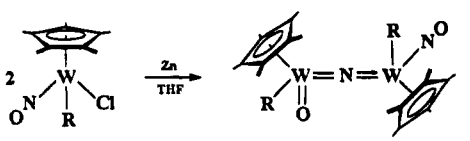

(1)

1 R = CH₂CMe₃
2 R = CH₂SiMe₃
3 R = Ph

Table 3. Fractional Coordinates (×10⁴) and Equivalent Isotropic Displacement Parameters (Å² × 10⁴) for the Non-hydrogen Atoms of [Cp*Mo(NO)(CH₂SiMe₃)](μ-N)-[Cp*Mo(O)(CH₂SiMe₃)] (5) at 190 K

atom	x	y	z	U_{eq}[a]
Mo(1)	1495.4(4)	75.0(3)	2264.9(2)	272
Mo(2)	4612.3(4)	−2375.2(3)	3023.4(2)	244
Si(1)	2874(1)	2453(1)	2310.0(7)	310
Si(2)	6756(1)	−3718(1)	1180.0(8)	393
O(1)	−437(4)	1709(4)	3751(2)	577
O(2)	5914(3)	−1728(3)	2779(2)	379
N(1)	494(4)	1044(4)	3179(2)	353
N(2)	3044(4)	−1304(3)	2639(2)	297
C(6)	2367(5)	1492(5)	1684(3)	363
C(7)	3847(7)	1510(5)	3084(4)	490
C(8)	4099(7)	3159(6)	1620(3)	549
C(9)	1154(6)	3858(5)	2856(4)	638
C(26)	5580(5)	−4014(4)	2135(3)	330
C(27)	5996(6)	−1979(6)	844(3)	534
C(28)	6931(7)	−4878(6)	367(3)	577
C(29)	8620(6)	−4114(7)	1332(4)	666
C(1)	−646(6)	683(5)	1779(3)	421
C(2)	412(6)	566(5)	1073(3)	419
C(3)	1468(6)	−749(5)	957(3)	431
C(4)	1020(5)	−1472(5)	1592(3)	373
C(5)	−279(5)	−604(6)	2142(3)	414
C(11)	−1993(7)	1894(6)	2126(5)	693
C(12)	404(8)	1630(7)	462(4)	661
C(13)	2708(7)	−1248(8)	202(4)	718
C(14)	1786(8)	−2959(5)	1661(5)	610
C(15)	−1202(8)	−995(8)	2845(4)	714
C(21)	4220(5)	−4067(4)	3961(2)	294
C(22)	5482(5)	−3908(4)	4070(2)	306
C(23)	5001(5)	−2597(4)	4369(2)	310
C(24)	3459(5)	−1932(4)	4423(2)	300
C(25)	2978(5)	−2866(4)	4193(2)	318
C(31)	4230(7)	−5362(5)	3730(3)	472
C(32)	7031(6)	−4965(5)	3924(3)	524
C(23)	5934(6)	−1980(6)	4584(3)	523
C(34)	2461(6)	−547(4)	4757(3)	436
C(35)	1414(5)	−2589(6)	4213(3)	513

[a] The equivalent isotropic displacement parameter is the cube root of the product of the principal axes of the anisotropic displacement ellipsoid.

Table 4. Selected Intramolecular Distances (Å) and Angles (deg) for [Cp*W(NO)(CH₂CMe₃)](μ-N)[Cp*W(O)Cl] (4) at 190 K

W(1)−N(1)	1.764(4)	W(2)−O(2)	1.714(4)
W(1)−N(2)	1.912(5)	W(2)−N(2)	1.808(5)
W(1)−C(6)	2.174(6)	W(2)−Cl	2.3382(19)
W(1)−C(1)	2.444(6)	W(1)−C(2)	2.379(7)
W(1)−C(3)	2.305(6)	W(1)−C(4)	2.387(6)
W(1)−C(5)	2.431(5)	W(1)−Cp1[a]	2.062
O(1)−N(1)	1.233(6)	W(2)−Cp2[b]	2.10
C(6)−C(7)	1.535(8)	C(7)−C(8)	1.505(9)
C(7)−C(9)	1.530(12)	C(7)−C(10)	1.522(9)
N(1)−W(1)−N(2)	99.93(22)	Cl−W(2)−O(2)	104.18(14)
N(1)−W(1)−C(6)	96.67(23)	Cl−W(2)−N(2)	101.26(13)
N(1)−W(1)−Cp1	121.8	Cl−W(2)−Cp2	110.2
N(2)−W(1)−C(6)	106.69(23)	O(2)−W(2)−N(2)	105.25(23)
N(2)−W(1)−Cp1	119.0	O(2)−W(2)−Cp2	116.1
C(6)−W(1)−Cp1	109.8	N(2)−W(2)−Cp2	118.0
W(1)−N(1)−O(1)	169.9(5)	W(1)−N(2)−W(2)	177.2(3)
W(1)−C(6)−C(7)	122.5(4)	C(8)−C(7)−C(9)	109.2(5)
C(6)−C(7)−C(8)	112.2(6)	C(8)−C(7)−C(10)	109.2(7)
C(6)−C(7)−C(9)	111.1(6)	C(9)−C(7)−C(10)	107.4(6)
C(6)−C(7)−C(10)	107.6(5)		

[a] Cp1 represents the center of mass of atoms C(1) through C(5). [b] Cp2 represents the center of mass (occupancy weighted) of atom sites C(21) through C(25) and C(41) through C(45).

A conversion of the type presented in eq 1 may also be utilized for the synthesis of another related ditungsten complex. Reduction of a 2:1 mixture of Cp*W(NO)(CH₂CMe₃)Cl and Cp*W(NO)Cl₂ in THF with elemental zinc affords [Cp*W(NO)(CH₂CMe₃)](μ-N)[Cp*W(O)Cl]

Table 5. Selected Intramolecular Distances (Å) and Angles (deg) for [Cp*Mo(NO)(CH_2SiMe_3)](μ-N)[Cp*Mo(O)-(CH_2SiMe_3)] (5) at 190 K

Mo—N(1)	1.769(4)	Mo(2)—O(2)	1.714(3)
Mo(1)—N(2)	1.908(3)	Mo(2)—N(2)	1.812(3)
Mo(1)—C(6)	2.171(4)	Mo(2)—C(26)	2.163(4)
Mo(1)—Cp1[a]	2.081	Mo(2)—Cp2[b]	2.097
Si(1)—C(6)	1.850(4)	Si(2)—C(26)	1.859(5)
Si(1)—C(7)	1.852(5)	Si(2)—C(27)	1.861(5)
Si(1)—C(8)	1.870(5)	Si(2)—C(28)	1.874(6)
Si(1)—C(9)	1.872(6)	Si(2)—C(29)	1.865(6)
O(1)—N(1)	1.203(5)		
Mo(1)—C(1)	2.368(5)	Mo(2)—C(21)	2.462(4)
Mo(1)—C(2)	2.474(5)	Mo(2)—C(22)	2.442(4)
Mo(1)—C(3)	2.469(5)	Mo(2)—C(23)	2.398(4)
Mo(1)—C(4)	2.390(4)	Mo(2)—C(24)	2.356(4)
Mo(1)—C(5)	2.297(4)	Mo(2)—C(25)	2.442(4)
N(2)—Mo(1)—N(1)	100.1(2)	N(2)—Mo(2)—O(2)	108.5(1)
C(6)—Mo(1)—N(1)	95.1(2)	C(26)—Mo(2)—O(2)	100.6(2)
C(6)—Mo(1)—N(2)	106.8(2)	C(26)—Mo(2)—N(2)	99.8(2)
N(1)—Mo(1)—Cp1	120.3	O(2)—Mo(2)—Cp2	116.6
N(2)—Mo(1)—Cp1	122.2	N(2)—Mo(2)—Cp2	118.6
C(6)—Mo(1)—Cp1	108.5	C(26)—Mo(2)—Cp2	110.0
C(7)—Si(1)—C(6)	115.8(2)	C(27)—Si(2)—C(26)	113.4(2)
C(8)—Si(1)—C(6)	108.8(2)	C(28)—Si(2)—C(26)	107.4(3)
C(8)—Si(1)—C(7)	107.2(3)	C(28)—Si(2)—C(27)	109.2(3)
C(9)—Si(1)—C(6)	108.5(3)	C(29)—Si(2)—C(26)	109.2(3)
C(9)—Si(1)—C(7)	107.7(3)	C(29)—Si(2)—C(27)	108.6(3)
C(9)—Si(1)—C(8)	108.7(3)	C(29)—Si(2)—C(28)	109.0(3)
O(1)—N(1)—Mo(1)	166.2(4)	Mo(2)—N(2)—Mo(1)	169.6(2)
Si(1)—C(6)—Mo(1)	119.2(2)	Si(2)—C(26)—Mo(2)	113.3(2)

[a] Cp1 represents the center of mass of atoms C(1) through C(5). [b] Cp2 represents the center of mass of atom sites C(21) through C(25).

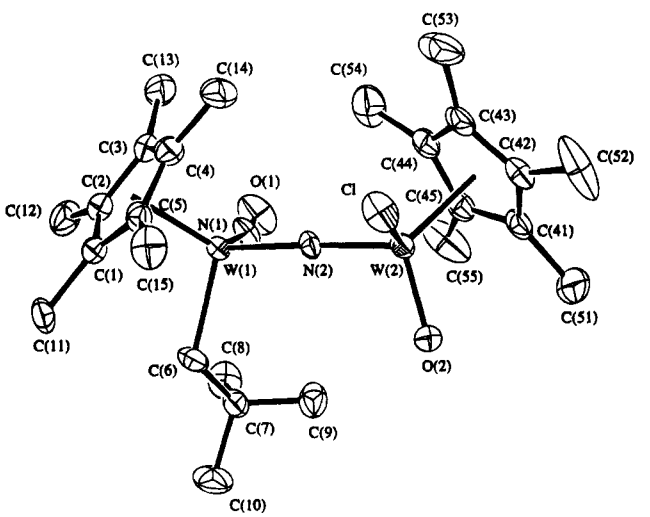

Figure 1. The solid-state molecular structure of **4**, 50% probability ellipsoids being shown for non-hydrogen atoms. For simplicity of presentation, only the major component of the disordered Cp* group on W(2) is shown.

(**4**) as analytically pure brown crystals in 24% isolated yield based on Cp*W(NO)Cl_2 (eq 2). The structure of **4** also provides some insight as to the probable mechanism of these reductions involving the tungsten complexes (vide infra).

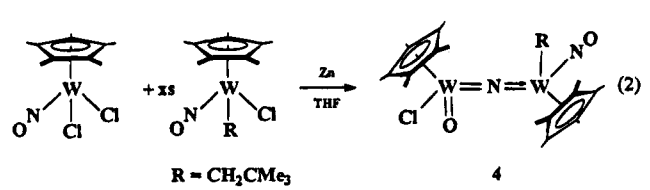

Bimetallic molybdenum complexes analogous to the tungsten congeners prepared via conversions 1 can be

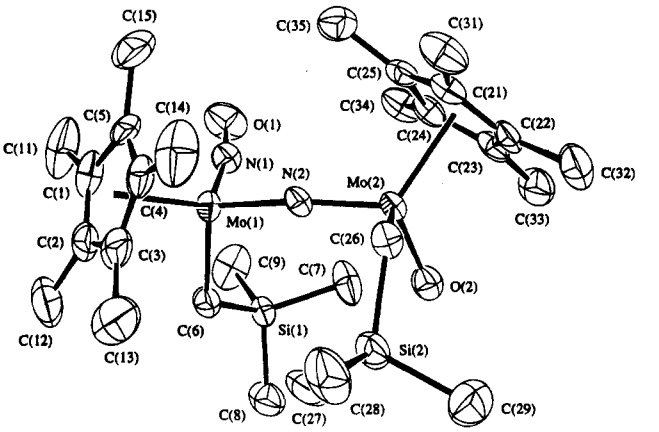

Figure 2. The solid-state molecular structure of **5**, 50% probability ellipsoids being shown for non-hydrogen atoms.

synthesized by the reaction of molecular hydrogen with the appropriate dialkyl precursors in benzene (eq 3).

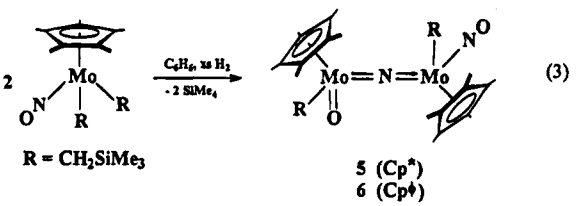

At present, the synthetic methods summarized in eqs 1 and 3 are specific to each of the tungsten and molybdenum systems, respectively. Our attempts to extend either methodology to encompass the other Group 6 congener have not yet met with success. Thus, a variety of Cp'W(NO)R_2 complexes react with H_2 to produce the well-known hydride dimers, [Cp'W(NO)-H_2]$_2$,[19] rather than the nitrido-bridged products as is observed for the molybdenum system.

The spectroscopic properties of complexes **1**–**6** are fairly similar. The ^{1}H NMR spectra of all six compounds in C_6D_6 display line-broadening in the signals assignable to the alkyl methylene protons. This broadening is invariant over the temperature range 20–50 °C and is probably a manifestation of the occurrence of hindered rotation of the alkyl groups about the CH_2—metal linkages, the bulkiness of the Cp* and other ligands on the adjacent metal being the primary cause of this effect. Consistently, this broadening is less severe in the spectrum of the complex having only one alkyl ligand, complex **4**, and most evident in the spectrum of **1**, the complex having the most sterically demanding environment at its metal centers.

The IR spectra of all four ditungsten complexes as Nujol mulls are remarkably similar and merit some comment. In addition to the diagnostic ν_{NO} bands that all of the complexes display in the normal region of 1500–1600 cm^{-1}, their spectra also exhibit sharp bands in the 800–960 cm^{-1} region. For instance, both tungsten complexes **1** and **2** display two sharp bands in their IR spectra at approximately 962 and 891 cm^{-1}, one being assignable to ν_{WO} and the other to ν_{asym}, the asymmetric stretching frequency of the M—N—M linkage. Other examples of similar tungsten oxo complexes which also show sharp bands in this region of the IR

(19) Legzdins, P.; Martin, J. T.; Einstein, F. W. B.; Willis, A. C. *J. Am. Chem. Soc.* **1986**, *108*, 7971.

spectrum include $Cp^*W(O)(Me)_2(CH_2SiMe_3)$ (ν_{WO} = 933 cm^{-1}) and $Cp^*W(O)(=CHPh)(CH_2SiMe_3)$ (ν_{WO} = 939 cm^{-1}).[4] Furthermore, similar ν_{asym} bands have been observed previously in the IR spectra of complexes such as $[NH_4]_3[(Br_5W)_2(\mu\text{-}N)]$ (ν_{asym} = 968 cm^{-1})[20] and $[Cp^*WMe_3]_2(\mu\text{-}N)$ (ν_{asym} = 800 cm^{-1}).[21] Labeling of the latter complex and its cationic analogue with ^{15}N results in a shift of this band to lower energy (e.g., for $[[Cp^*WMe_3]_2(\mu\text{-}N)]PF_6$ from 999 to 969 cm^{-1}), thereby supporting its assignment to a W–N stretching mode. In contrast to the ditungsten complexes **1–4**, the IR spectra of the dimolybdenum complexes **5** and **6** exhibit more than two bands in the 960–800 cm^{-1} region, thereby precluding their ready assignment to specific vibrational modes.

X-ray Crystallographic Analyses of $[Cp^*W(NO)(CH_2CMe_3)](\mu\text{-}N)[Cp^*W(O)Cl]$ (4) and $[Cp^*Mo(NO)(CH_2SiMe_3)](\mu\text{-}N)[Cp^*Mo(O)(CH_2SiMe_3)]$ (5). The solid-state molecular structures of **4** and **5** are shown in Figures 1 and 2, respectively. For clarity of presentation, only the major orientation of the disordered Cp* group in complex **4** is shown. There are no intermolecular distances significantly shorter than the appropriate sums of accepted Van der Waals radii in either structure.

The most chemically interesting feature about the solid-state molecular structures of **4** and **5** is the orthogonal orientation of the metal-containing units about the essentially linear M–N–M (M = Mo, W) bridging linkages, an aspect consistent with the existence of multiple bonding in these links (vide infra). The nearly linear M–N–M arrangements [Mo(1)–N(2)–Mo(2) = 169.6(2)°; W(1)–N(2)–W(2) = 177.2(3)°] display some asymmetry in the bond lengths to the central nitrogen atom, this asymmetry being reflective of the differing electronic environments at the two metal centers. Nevertheless, these metal–nitrogen distances [i.e., Mo(1)–N(2) = 1.908(3) Å, Mo(2)–N(2) = 1.812(3) Å; W(1)–N (2) = 1.912(5) Å, W(2)–N(2) = 1.808(5) Å] are similar in length to the W–NCHMe bond distance in $Cp^*W(NO)(CH_2SiMe_3)(N{=}CHMe)$ (~1.9 Å; disorder in the latter structure prevented a more precise determination) and related structures.[22] Such a comparison suggests that the W(1)–N(2) linkage in **4** and the Mo(1)–N(2) bond in **5** are double bonds similar in character to that extant in the tungsten ethylideneamido complex. Further comparisons of these bonds can be made to the analogous link in $[Cp^*WMe_3]_2(\mu\text{-}N)$ which has a symmetric, linear W–N–W bridge with W–N bond lengths of 1.8475(8) Å.[23]

The tungsten–oxygen bond in **4** is of a typical length [1.713(4) Å] and can be compared to the similar bond distances in $CpW(O)_2(CH_2SiMe_3)$ [1.723(5) and 1.716(5) Å].[24] Consistently, the Mo(2)–O(2) separation in **5** is 1.714(3) Å. In valence-bond terms, the bonding in the central M–N–M linkages of these bimetallic complexes may be represented pictorially as shown in eqs 1–3. Such representations suggest that the metal center bearing the NO ligand attains an 18-valence-electron configuration whereas that bearing the oxo ligand has 16 valence electrons. However, the bimetallic complexes do not react with Lewis bases once they are formed, and they are stable as solids in air for at least a number of days. Consequently, it is probably best to view complexes **4** and **5** as containing electronically saturated metal centers, with the formally 16-valence-electron center probably attaining additional electron density from the oxo ligand.

In addition to displaying analogous stereochemistry, the molecules of **4** and **5** are very similar in their finer features as well. In both molecules the relative torsional dispositions of the two Cp* groups about the M–M axis are nearly perpendicular [Cp1–Mo(1)–Mo(2)–Cp2 = 99.4°; Cp1–W(1)–W(2)–Cp2 = 101°; where Cp1 and Cp2 represent the respective centers of mass of the cyclopentadienyl rings]. Likewise, the two "one-electron ligands" (alkyl or Cl) in each case, as well as the NO and O ligands, are similarly related [i.e., N(1)–Mo(1)–Mo(2)–O(2) = 93.7(2)°, C(6)–Mo(1)–Mo(2)–C(26) = 101.3(2)°, C(6)–W(1)–W(2)–Cl = 104.7(1)°, N(1)–W(1)–W(2)–O(2) = 96.1(2)°]. One feature of this arrangement is that, in either case, the oxo ligand eclipses the alkyl group on the opposing metal center when the molecules are viewed along the M–M axis [C(6)–Mo(1)–Mo(2)–O(2) = 3.4(2)°; C(6)–W(1)–W(2)–O(2) = 3.6(2)°]. The orthogonal relationship of the end groups suggests that the M=N=M bonding interaction involves orthogonal p orbitals on the central N atom for the formation of the π bonds to the metals in a manner analogous to that found for related oxo-bridged species.[13] That electronically similar ligands are found to be oriented mutually perpendicularly is, at least intuitively, reasonable. In this connection, it is interesting to note that we do not have any evidence for the existence of diastereomers of complexes **4** and **5** such as those that would result, for example, if the alkyl and NO ligands on M(1) were interchanged.

Probable Mechanism of Formation of the Bimetallic Complexes. A plausible mechanism that accounts for the formation of the bimetallic tungsten complexes isolated during this work is presented in Scheme 1. Initial reduction of $Cp'W(NO)(R)(Cl)$ (R = alkyl or aryl) by zinc results in the formation of the corresponding anion, which subsequently expels Cl^- to form the $Cp'W(NO)(R)$ radical which may or may not have the nitrosyl ligand coordinated in an η^2 fashion to the electron-deficient metal center. This radical could then combine with another equivalent of the starting material in a Lewis acid–base manner to form a bimetallic intermediate having a bridging η^2-NO group. Reduction followed by subsequent rearrangement would form the final product. The key feature of this mechanism is that it is the complex which is reduced first that undergoes subsequent nitrosyl N–O bond cleavage. Consistently, treatment of a 2:1 mixture of $Cp^*W(NO)(CH_2CMe_3)Cl$ and $Cp^*W(NO)Cl_2$ in THF with zinc powder affords the related bimetallic complex $[Cp^*W(NO)(CH_2CMe_3)](\mu\text{-}N)[Cp^*W(O)Cl]$ (**4**) in 24% isolated yield. The oxo ligand in **4** is on the metal center bearing the chloro ligand, as expected on the basis of the mechanism summarized in Scheme 1, since we have previously established by cyclic voltammetry that $Cp^*W(NO)Cl_2$ is more easily reduced than $Cp^*W(NO)(CH_2$-

(20) Hörner, M.; Frank, K.-P.; Strähle, J. *Z. Naturforsch.* **1986**, *41b*, 423.
(21) Glassman, T. E.; Liu, A. H.; Schrock, R. R. *Inorg. Chem.* **1991**, *30*, 4732.
(22) Debad, J. D.; Legzdins, P.; Batchelor, R. J.; Einstein, F. W. B. *Organometallics* **1992**, *11*, 6 and references therein.
(23) Glassman, T. E.; Vale, M. G.; Schrock, R. R. *Organometallics* **1991**, *10*, 4046.
(24) Legzdins, P.; Rettig, S. J.; Sánchez, L. *Organometallics* **1985**, *4*, 1470.

Scheme 1

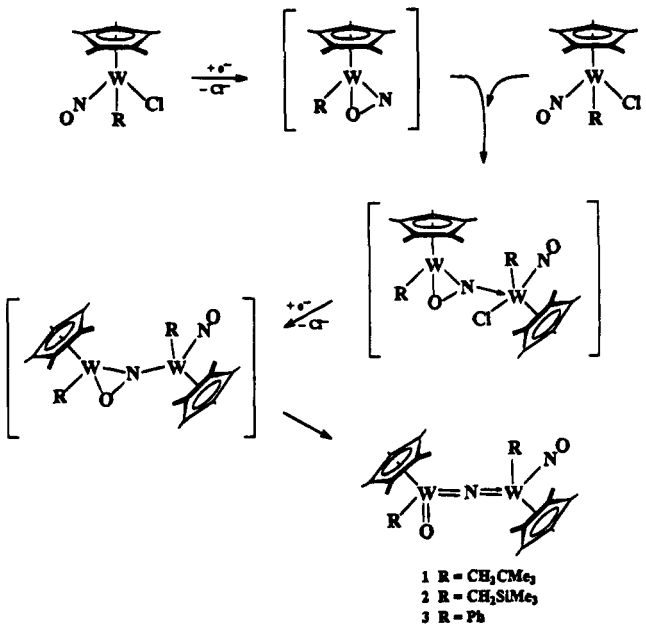

CMe_3)Cl.[25] In other words, the formation of [Cp*W(NO)(CH_2CMe_3)](μ-N)[Cp*W(O)Cl] proceeds via attack of the transient Cp*W(η^2-NO)Cl on the excess Cp*W(NO)(CH_2CMe_3)Cl.

In the case of the molybdenum systems, reaction of Cp'Mo(NO)$(R)_2$ with molecular hydrogen probably generates the transient hydride, Cp'Mo(NO)(R)(H),[26] which could then combine with another equivalent of Cp'Mo(NO)$(R)_2$ with intermolecular elimination of RH to form a bimetallic intermediate having a bridging η^2-NO group analogous to that invoked in the tungsten case. This intermediate could then subsequently rearrange to the final dimolybdenum product.

Acknowledgment. We are grateful to the Natural Sciences and Engineering Research Council of Canada for support of this work in the form of grants to P.L. and F.W.B.E. and a postgraduate scholarship to J.D.D. We also thank the University of British Columbia for the award of a University Graduate Fellowship to M.A.Y. and the Spanish Ministry of Education for the award of a postdoctoral fellowship to R.R.

Supplementary Material Available: Additional crystallographic data for complexes **4** and **5**, including tables of experimental details, hydrogen atom parameters, anisotropic thermal parameters, bond distances and angles, torsion angles, and least-squares planes (19 pages). Ordering information is given on any current masthead page.

OM9403232

(25) Debad, J. D.; Legzdins, P.; Rettig, S. J.; Veltheer, J. E. *Organometallics* **1993**, *12*, 2714.

(26) This hydride may be trapped with acetone to obtain Cp'Mo(NO)(R)$OCHMe_2$); Legzdins, P.; Young, M. A. Unpublished observations.